JOURNAL OF SOLID STATE CHEMISTRY 114, 311–316 (1995)

Manganese(II,III) Oxyborate, Mn_2OBO_3: A Distorted Homometallic Warwickite—Synthesis, Crystal Structure, Band Calculations, and Magnetic Susceptibility

R. Norrestam,[1] M. Kritikos, and A. Sjödin

Department of Structural Chemistry, Arrhenius Laboratory, Stockholm University, S-10691 Stockholm, Sweden

Received October 28, 1993; in revised form March 7, 1994; accepted March 9, 1994

The manganese(II,III) oxyborate with the composition Mn_2OBO_3 has been synthesized by high-temperature techniques. X-ray studies show that crystals of the specimen, grown with borax as flux, are monoclinic, with space group $P2_1/n$, $a = 9.2866(7)$, $b = 9.5333(10)$, $c = 3.2438(3)$ Å, and $\beta = 90.757(7)°$. A model of the crystal structure has been refined with the 2064 most significant ($I \geq 5 \cdot \sigma_I$) X-ray reflections with $\sin(\theta)/\lambda \leq 1.08$ Å^{-1} to $R = 0.40$. The structure of Mn_2OBO_3 can be considered to be a distorted modification of the orthorhombic warwickite structure. The distortions, apparently caused by Jahn–Teller effects induced by the Mn^{3+} ions, remove the mirror symmetry of the parent undistorted warwickite. As a consequence, the space group symmetry is lowered from *Pnam* to one of its subgroups, $P2_1/n$. The structural results as well as the measured magnetic susceptibilities indicate high-spin manganese ions. The magnetic susceptibilities in the temperature region 110–300 K follow the Curie–Weiss law. The Weiss constant of −132(1) K indicates an antiferromagnetic ordering at low temperature. The bond distances and calculated bond valence sums indicate that the trivalent manganese ions are located in the two inner columns of the four-octahedra-wide walls. This metal charge distribution is supported by extended Hückel band calculations on some homometallic warwickites. The difference in metal coordination around one of the borate oxygen atoms is reflected by a significant deviation of the borate group geometry from the ideal trigonal symmetry.

INTRODUCTION

Metal-rich anhydrous oxyborates, containing six-coordinated metal ions of mixed valences, frequently adopt the warwickite or any of the pinakiolite types (1) of structures (e.g., ludwigite). The metal : boron ratio of warwickite is 2 : 1, while the pinakiolite type has a ratio of 3 : 1. For mixtures of divalent (M') and trivalent (M'') metal ions, the compositions would be $M'M''OBO_3$ and $M'_2M''O_2BO_3$, respectively. For transition metals, e.g., iron, cobalt and manganese, that can form compounds with mixed valences in the solid state, homometallic oxyborates with the warwickite and/or the pinakiolite type of structures can be anticipated. Known homometallic examples include $Fe_3O_2BO_3$ (2) and $Co_3O_2BO_3$ (3), both crystallizing with a ludwigite type of structure.

The warwickite structure is not confined only to metal oxyborates. Thus, beryllates such as Y_2OBeO_3 (4) have structures similar to warwickite. Remarkably, even some chalcogenides (S or Se) adopt a structure, known as the Yb_3S_4 type (5, 6), that can be considered to be related to warwickite. The compositional relation to warwickite becomes more obvious if the chemical formula of these chalcogenides is written as $M'M''SM''S_3$, with *inter alia* $M' = Yb^{2+}$, Ca^{2+}, and $M'' = Yb^{3+}$.

The present study concerns a new synthetic manganese oxyborate with a warwickite composition. Distorted coordination octahedra around the Mn^{3+} ions can be expected to originate from the Jahn–Teller effect. Consequently, the high Mn^{3+} content in the present case can be expected to lead to new modifications of the warwickite structure (7).

SYNTHESIS

The manganese(II,III) oxyborate can be prepared when manganese(III) oxide (α-Mn_2O_3) is thermally decomposed at 800° in air, in the presence of boron(III) oxide (B_2O_3). The α-Mn_2O_3 is easily prepared from commercial MnO_2 by annealing in air at 800°C for a few hours (see, e.g., Ref. 8). A mixture of Mn_2O_3 and B_2O_3 was annealed at 800°C for 4 days, cooled to room temperature, powdered, and then annealed again for another 4 days. After this treatment the product still contained some unreacted Mn_2O_3. By using an alternative preparation route, with $Mn(NO_3)_2 \cdot 4H_2O$ and H_3BO_3 as starting materials, almost pure manganese(II,III) oxyborate is obtained when a mixture (stoichiometric ratio 2 : 1) is annealed at 700°C for 3 days. The manganese oxyborate specimen was recrystallized by using borax flux. To obtain crystals of sizes suit-

[1] To whom correspondence should be addressed.

0022-4596/95 $6.00

able for single crystal X-ray diffraction studies, a mixture (weight ratio 1 : 1) of the oxyborate and borax was heated to 1000°C in air for 10 hr, followed by cooling (30°/hr) to 600°C before the furnace was turned off.

X-ray powder photographs on the various manganese oxyborate specimens indicated that the only borate formed was the manganese(II,III) oxyborate, Mn_2OBO_3, of warwickite composition. No powder diffraction lines that could indicate the presence of either a simple trivalent borate, e.g., $MnBO_3$, or any borate with pinakiolite composition ($Mn_3O_2BO_3$) could be observed. It could be noted that when preparing iron (2) or cobalt (3) oxyborate, and applying synthetic procedures similar to those described above, the simplest member of the pinakiolite family, ludwigite, is obtained. Attempts that were especially focused on preparation of *inter alia* $MnBO_3$ or $Mn_3O_2BO_3$, by using related synthetic procedures, have not been successful so far.

EXPERIMENTAL

Needle-shaped black crystals were selected from the synthesized specimen. The intensity distribution on single crystal X-ray photographs, using de Jong and precession techniques, indicated the space group symmetry $P2_1/n$ and unit cell dimensions typical for the warwickite structure type. The nonstandard-oriented space group was selected rather than the standard one ($P2_1/c$), in order to give unit cell dimensions and atomic coordinates that are easily comparable to those of common orthorhombic (*Pnam*) warwickite. The space group $P2_1/n11$ is a subgroup of *Pnam* (see discussion below), but as the *b* axis is chosen as the monoclinic axis, the results of the present study must be compared with a **bac̄** orientation of the structural data for orthorhombic warwickites. From a Guinier X-ray powder photograph, the cell parameters obtained by least-squares methods, using 18 uniquely indexed line positions, were $a = 9.287(1)$, $b = 9.536(1)$, $c = 3.2456(6)$ Å, and $\beta = 90.74(1)°$. The close agreement with the parameters determined for the single crystal (cf. Table 1), which was used for data collection, ensures that the selected crystal was representative of the whole specimen.

Single crystal X-ray diffraction data were collected at room temperature and corrected for background Lorentz, polarization, and absorption effects. Further relevant experimental data are listed in Table 1. Initial atomic coordinates of the metal positions were derived from an interpretation of a calculated Patterson map, and the coordinates of the oxygen and boron atoms were deduced from subsequent difference electron density ($\Delta\rho$) maps. The coordinates were, as expected (see discussion above), to be close to those of **bac̄**-oriented orthorhombic common warwickite. To avoid local least-squares minima in the structure model refinements, the z parameters of the atoms were allowed to deviate slowly and stepwise from the initial value $z = \frac{1}{4}$. Due to the very small differences in X-ray scattering powers between Mn^{2+} and Mn^{3+} ions, attempts to obtain information on the $Mn^{2+} : Mn^{3+}$ ratio at the two symmetry-independent metal positions from the diffraction data failed.

The final atomic coordinates and thermal parameters are given in Table 2, and the most relevant interatomic distances and angles are given in Table 3. The atomic labeling used is similar to that used in a previous study (7) of the warwickite structure type. The structural refinements were performed with the SHELX-76 program package (9). The atomic scattering factors in the final refinement stage were those of neutral atoms from the

TABLE 1
Experimental Details of the Crystal Structure Determination of Mn_2OBO_3

Formula	Mn_2OBO_3
Formula weight	184.68
Space group	$P2_1/n$
Unit cell dimensions	$a = 9.2866(7)$, $b = 9.5333(10)$, $c = 3.2438(7)$ Å, and $\beta = 90.757(7)°$
Unit cell volume, V	287.2(1) Å^3
Formula units per unit cell, Z	4
Density (calc), d_x	4.271(2) g · cm^{-3}
Radiation	Mo$K\alpha$
Wavelength, λ	0.71073 Å
Temperature, T	293(1) K
Crystal shape	Prismatic
Crystal size	0.07 × 0.12 × 0.60 mm
Diffractomer	CAD 4
Intensity data collection:	ω-θ scan
Maximum $\sin(\theta)/\lambda$	1.08 Å^{-1}
Range of h, k, and l	$-19 \le h \le 19$, $0 \le k \le 20$, and $0 \le l \le 6$
Internal R	0.014
Collected reflections	3282
Unique reflections	2976
Observed reflections	2064
Criterion for significance	$5 \cdot \sigma_I$
Absorption correction:	Numerical integration
Linear absorption coefficient	82.7 cm^{-1}
Transmission factor range	0.32–0.67
Structure refinement:	Full-matrix least-squares
Minimized function	$\Sigma w \cdot (\Delta F)^2$
Anisotropic thermal parameters for	Mn and O
Isotropic thermal parameter for	B
Number of refined parameters	60
Weighting scheme	$(\sigma_{F^2} + 0.0007\lvert F^2\rvert)^{-1}$
R for observed reflections	0.040
wR for observed reflections	0.053
Max of $\lvert\Delta\rvert/\sigma$	0.002
Max and min of $\Delta\rho$	3.9 and −3.2 $e \cdot$ Å^{-3}

TABLE 2
Fractional Atomic Coordinates ($\times 10^4$) and Isotropic Thermal Parameters ($\times 10^4$ Å^2) for the Mn_2OBO_3 structure

Atom	x	y	z	U_{eq}/U_{iso}
Mn(1)	5573.3(.3)	3836.4(.3)	−2147(1)	52(1)
Mn(2)	1701.0(.3)	4028.0(.3)	−2205(1)	73(1)
O(1)	1127(1)	−92(1)	−2850(5)	65(3)
O(2)	−122(1)	2511(2)	−1344(5)	78(3)
O(3)	7287(1)	2612(2)	−1739(5)	75(3)
O(4)	8719(2)	4655(2)	−2771(5)	82(3)
B	8617(2)	3272(2)	−1923(6)	55(3)

Note. The esd's are given in parentheses. The equivalent isotropic thermal parameters of the anisotropically refined metal and oxygen atoms, were estimated as $\frac{1}{3} \cdot \text{trace}(U)$.

TABLE 3
Relevant Metal–Oxygen Distances (d_{M-O}) and Oxygen–Metal–Oxygen Angles (for $d_{M-O} < 2.5$ Å) in the Mn_2OBO_3 Structure

Atoms		d_{M-O} (Å)	Atoms		d_{M-O} (Å)
Mn(1)–O(1)		2.269	Mn(2)–O(1)		2.185
O(1)		1.904	O(2)		2.247
O(1)		1.881	O(3)		2.220
O(2)		1.975	O(3)		2.421
O(2)		2.376	O(4)		2.090
O(3)		1.977	O(4)		2.086
O(4)		3.034	O(4)		2.837
B–O(2)		1.388			
O(3)		1.388			
O(4)		1.350			
Atoms		**Angle (°)**	**Atoms**		**Angle (°)**
O(1)–Mn(1)–O(1)	*	82.9	O(1)–Mn(2)–O(2)		160.6
O(1)	*	85.0	O(3)		92.4
O(1)		101.7	O(3)		92.4
O(2)	*	80.5	O(4)		86.5
O(2)	*	81.7	O(4)		86.8
O(2)		93.2	O(2)–Mn(2)–O(3)	*	69.9
O(2)		95.0	O(3)	*	79.7
O(2)		175.8	O(4)		98.2
O(2)		177.0	O(4)		110.5
O(3)		96.5	O(3)–Mn(2)–O(3)		88.6
O(3)		100.1	O(4)	*	82.2
O(3)		174.9	O(4)	*	87.2
O(2)–Mn(1)–O(2)		96.0	O(4)		170.7
O(3)	*	81.7	O(4)		175.6
O(3)	*	85.3	O(4)–Mn(2)–O(4)		101.9
O(2)–B–O(3)		120.4			
O(4)		118.5			
O(3)–B–O(4)		121.1			

Note. The angles involving oxygen atoms that form shared edges between adjacent coordination octahedra are marked with an asterisk. The esd's for distances and angles involving Mn are about 0.001 Å and 0.1°, respectively, and those involving B are about 0.002 Å and 0.3°.

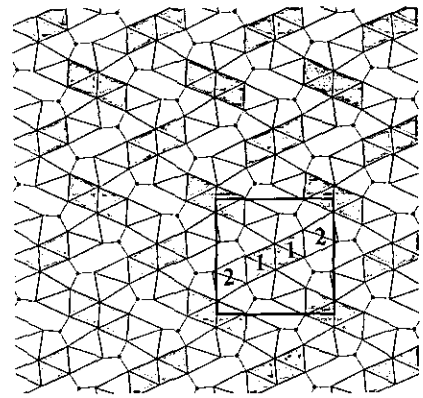

FIG. 1. Polyhedral representation of the Mn_2OBO_3 warwickite structure viewed along the c axis. Coordination octahedra around the Mn(1) positions (labeled 1) are gray and those around the Mn(2) positions (labeled 2) are light gray. The unit cell and the metal atom numbering are indicated. The b axis is horizontal, the a axis is vertical and the origin is at the upper left corner. The boron atom positions are drawn as filled circles and boron–oxygen bonds are indicated by single lines.

International Tables for X-ray Crystallography (10). The program ATOMS (11) was utilized to obtain the structure diagrams.

Electronic band calculations were performed using the semiempirical extended Hückel tight-binding method (EHTB), using the program (QCPE No. 571) written by Whangbo *et al.* (12). Sets of k-points, uniformly distributed in the irreducible part of the Brillouin zone, were selected by the scheme developed by Monkhorst and Pack (13); 128 and 64 k-points were used in the monoclinic and orthorhombic warwickite modifications, respectively.

The magnetic susceptibility of a powder sample of Mn_2OBO_3, in the temperature range 14–325 K, was measured by using a Lake Shore AC susceptometer Model 7130 equipped with a helium cryostat. Measurements on tetramethylethylene-diammonium tetrachlorocuprate(II), $[(CH_3)_2NHCH_2CH_2NH(CH_3)_2]CuCl_4$, were used (14) to check the performance of the susceptometer. A frequency of 500 Hz and a magnetic field strength of 500 A $\cdot$ m^{-1} were used.

CRYSTAL STRUCTURE

The general features of the crystal structure (Fig. 1) agree with the previously determined structures of the warwickite type (1, 7, 15, 16). Thus, the manganese atoms are approximately octahedrally coordinated by oxygen atoms. The coordination octahedra are linked by edge sharing to form four-octahedra-wide flat walls, which extend along [001]. The walls are linked together by edge sharing into a herringbone pattern. The planar trigonal borate groups are located in the voids between the walls and attached to them by corner sharing (Fig. 1). Two

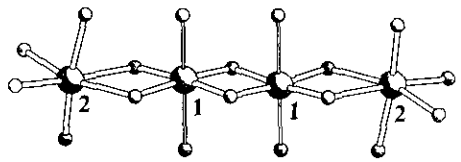

FIG. 2. Coordinations around the manganese atoms across the four-octahedra-wide walls in Mn_2OBO_3. The numbers shown are the numeric labels of the manganese positions. The two inner metal atoms are the Mn(1) and the two outer ones are the Mn(2) positions. Atoms are related by an inversion center at the center of the figure. The two longer Mn–O bonds of 2.269 and 2.376 Å (see Table 3) at each of the Mn(1) positions are vertical and drawn with thinner bonds.

columns of coordination octahedra around the Mn(2) positions form the outer two columns of the walls and two octahedra columns around the Mn(1) positions form the inner two columns (see Fig. 2).

Experimentally determined distributions (6, 15) of di- and trivalent metal ions have shown that trivalent ions prefer the $M(1)$ positions (Mn(1) in the present case) and that divalent ions prefer the $M(2)$ positions (Mn(2)). For, e.g., $MgScOBO_3$, the contents of Sc^{3+} at the $M(1)$ and of Mg^{2+} at the $M(2)$ positions are 76(1)%. In the present study, the similarity of the X-ray powder scattering does not permit any determination of the $Mn^{2+}:Mn^{3+}$ ratios from the diffraction data. Indications of the ion distributions at the metal positions can however be obtained with empirical correlation functions, relating bond lengths to bond valences. Brown and Altermatt (17) have estimated the parameters for such functions from a wide variety of structural data. With the parameters for Mn^{2+} the bond valence sums (bvs) for the Mn(1) and Mn(2) positions, summed over the six shortest Mn–O bonds (Table 3) at each position, become 3.21 and 2.02 valence units (v.u.), respectively. With the Mn^{3+} parameters the corresponding bvs values become 2.96 and 1.86 v.u. The values suggest that the Mn(1) and Mn(2) positions are occupied by approximately pure trivalent and divalent manganese, respectively. Although the ion valence distribution deviates from that observed in a common undistorted warwickite such as $MgScOBO_3$ (7), it agrees with the metal composition at the metal sites of the Mn^{3+}-containing (and distorted) warwickite $Mg_{0.76}Mn_{1.24}OBO_3$ (7). One reason that the Mn^{3+} content is located in the Mn(1) positions in the two Mn^{3+}-containing warwickites is probably related to the preference (caused by the Jahn–Teller effect) for high-spin Mn^{3+} to have an axially elongated octahedral oxygen-coordination geometry. Changes of the coordination geometry appear to be more geometrically restricted at the Mn(2) position than at the Mn(1) position, by the presence of the two very short Mn(2)–O(4) bonds. Such short $M(2)$–O(4) bonds are common features of all warwickites (see below). The bond length distributions at the Mn(1) and Mn(2) positions further support the conclusion that these positions are occupied by trivalent and divalent manganese, respectively. It has been shown (18) that by using root of harmonic mean square (rhms) values $(r_0 = [\frac{1}{6}\Sigma\, 1/(d_i - 1.40)^2)]^{-1/2}$, where 1.40 is an estimate of the oxygen radius (in Å) to estimate ion radii (r_0) from bond distances (d_i), the estimates are independent of the degree of distortion of the coordination octahedra. This is not the case if the radii are estimated as, e.g., average or root mean square values. In the present case the manganese–oxygen distances give the estimated rhms radii of 0.60 and 0.79 Å (average radii 0.66 and 0.81 Å) for the Mn(1) and Mn(2) atoms, respectively. The value for Mn(1) agrees well with the value 0.59(1) Å, recently estimated for Mn^{3+} (18). The average value, 0.81 Å, for Mn(2) is only slightly lower than the radius, 0.83 Å, of high-spin Mn^{2+} given by Shannon (19). Some of the distortions of the coordination octehedra can be ascribed to the common structural effects (20) that occur when adjacent coordination octahedra share an edge. Thus, the O–Mn–O bond angles formed at the manganese positions, that involve two edge-defining oxygen atoms are less than 90°, ranging from 69.9° to 87.2° (Table 3).

When compared to ordinary undistorted warwickites, the distortions of the present Mn_2OBO_3 structure and of the $Mg_{0.76}Mn_{1.24}OBO_3$ structure (7) involve lowering the space group symmetry. In these warwickites, the space group symmetry is *Pnam*, with all atoms located in the mirror planes at $z = \pm\frac{1}{4}$. As the distortions remove the mirror symmetry of the coordination octahedra, especially around Mn(1), it can be anticipated that the obtained space group symmetries would be one of the monoclinic subgroups of *Pnam*. The maximal nonisomorphic monoclinic subgroups (cf. 21) without symmetry elements along [001] are, when written with full Hermann–Maugin symbols, $P2_1/n11$ and $P12_1/a1$. In the former subgroup the

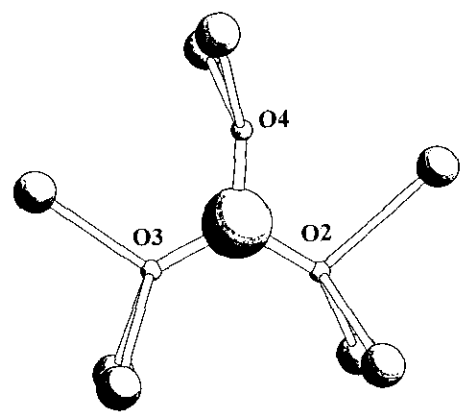

FIG. 3. Metal coordination around the oxygen atoms of the borate groups in Mn_2OBO_3. The numbers shown are the numeric labels of the borate oxygen atoms.

n-glide of *Pnam* is preserved and in the latter the *a*-glide. Thus, the structures of the two synthetic manganese warwickites, Mn_2OBO_3 ($P2_1/n$) and $Mg_{0.76}Mn_{1.24}OBO_3$ ($P2_1/a$), represent examples of each of the two anticipated monoclinic symmetry subgroups of *Pnam*.

The precision obtained in the present study, e.g., B–O bond lengths determined with esd's of 0.002 Å, permits a detailed analysis of the geometry of the borate ion that can be expected to be valid also for other warwickites. The observed distances and angles indicate that the borate ion geometry deviates significantly from that of ideal trigonal symmetry. The main source of the deviations is obviously the different metal coordination around one (O(4)) of the three borate oxygen atoms in the warwickite structure (cf. 7). Two of the borate oxygen atoms, O(2) and O(3), are three-coordinated by metal ions (Fig. 3) and both B–O distances are 1.388 Å. The third oxygen atom, O(4), which is only two-coordinated by metal ions (two divalent Mn(2) atoms), participates in a short B–O bond, 1.351 Å, and the two Mn(2)–O(4) bonds are also short. The Mn(2)–O(4) bond distances, about 2.09 Å, could be compared to the expected average Mn^{2+}–O^{-2} bond distance, which from empirical ionic radii (19) for high-spin Mn^{2+} and three-coordinated O^{-2} ions is estimated to be 2.19 Å. The oxygen–boron–oxygen angles in the borate group (Table 3) deviate significantly from the ideal trigonal value of 120°. The O(4) atom is displaced from its ideal position, away from the adjacent Mn(2) atoms, to give the O(2)–B–O(4) angle a value of 118.5°, significantly less than 120° (Fig. 3). Calculations of bvs values for the three borate oxygen atoms give values of 1.99 to 2.01 v.u., in agreement with the formal oxygen valence of −2.00.

In order to get some qualitative picture of the charge distributions at the different metal sites, semiempirical

TABLE 5

Overlap Populations (OP) for *M*–O (*M*=Fe and Co) and B–O Interactions with Calculated Charges for Fe, Co, O, and B in Fe_2OBO_3 and Co_2OBO_3 (in the $FeCoOBO_3$ Geometry)

M–O	Distance (Å)	OP(Fe)	OP(Co)
M(1)–O(1)	2.004	0.27	0.25
M(1)–O(1)	2.012	0.27	0.25
M(1)–O(2)	2.160	0.18	0.16
M(1)–O(3)	2.088	0.22	0.19
M(2)–O(1)	1.964	0.33	0.30
M(2)–O(2)	2.118	0.20	0.19
M(2)–O(3)	2.163	0.18	0.15
M(2)–O(4)	2.016	0.25	0.21
B–O(2)	1.389	0.67	0.67
B–O(3)	1.397	0.66	0.66
B–O(4)	1.354	0.69	0.70
	Atom	Charge	
	Fe(1)	1.07	
	Fe(2)	0.80	
	O(1)	−0.73	
	O(2)	−0.86	
	O(3)	−0.85	
	O(4)	−0.90	
	B	1.47	
	Co(1)	1.06	
	Co(2)	0.93	
	O(1)	−0.77	
	O(2)	−0.85	
	O(3)	−0.88	
	O(4)	−0.95	
	B	1.47	

Note. The OPs were evaluated at the highest occupied crystal orbital and normalized to one bond.

TABLE 4

Extended Hückel Parameters

Atom	Orbital	H_{ii}	ζ_1	c_1	ζ_2	c_2
B	2*s*	−15.2	1.3			
	2*p*	−8.5	1.3			
O	2*s*	−32.3	2.275			
	2*p*	−14.8	2.275			
Co	4*s*	−9.21	2.0			
	4*p*	−5.29	2.0			
	3*d*	−13.18	5.55	(0.5680)	2.10	(0.6060)
Fe	4*s*	−9.10	1.9			
	4*p*	−5.32	1.9			
	3*d*	−12.6	5.35	(0.5505)	2.00	(0.6260)
Mn	4*s*	−9.75	1.9			
	4*p*	−5.89	1.9			
	3*d*	−11.67	5.15	(0.5139)	1.70	(0.6929)

Note. H_{ii} is the effective potential (eV), ζ is the Slater-type orbital exponents, and c is the coefficients used in double Z-expansion.

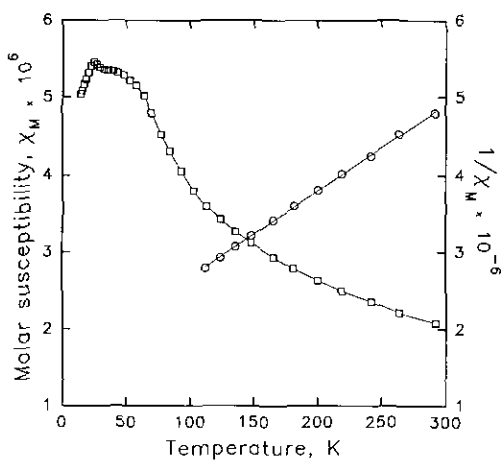

FIG. 4. Temperature dependence (14–300 K) of the molar magnetic susceptibility (squares), χ_M, together with the least-squares fit of the inverse susceptibility (circles) for the high-temperature region (110–300 K).

extended Hückel (EH) electronic band calculations were performed. Standard values of the EH parameters (22), without charge iteration, were used throughout all calculations (see Table 4). The use of charge iterations has been advocated by, e.g., Pyykkö (23), as this procedure would give a more realistic description of charges in inorganic solids. However, a qualitative estimate of charge distribution among different metal atom sites can usually (see, e.g., Ref 24) be obtained even without charge iteration. Two warwickite modifications were investigated, the present monoclinic manganese compound, Mn_2OBO_3, and the undistorted orthorhombic Fe,Co-warwickite, $FeCoOBO_3$ (16). In the latter compound, the metals at the cobalt positions were changed to iron and vice versa, to make the homometallic warwickite models Fe_2OBO_3 and Co_2OBO_3 more suitable for calculations. The EHTB calculations on Mn_2OBO_3 gave charges of +2.2 at the $M(1)$ and −0.1 at the M(2) positions. Although these charges have unrealistic values (possibly due to the absence of charge iteration), they indicate charge separation between the two sites. The calculations on the Fe_2OBO_3 and Co_2OBO_3 models are in general agreement (Table 5) with each other and suggest a similar, but smaller, metal charge separation. Concerning Mn_2OBO_3, the chemical significance of the absolute values of these charges are limited. The three-coordinated oxygen atom O(4) gets a large negative charge, which deviates significantly from those of the four-coordinated borate oxygen atoms, O(2) and O(3). As anticipated, the metal–oxygen overlap populations (Table 5) are highly correlated to the bond distances. The calculations do not indicate any direct metal–metal interactions in the structures.

The molar susceptibility, χ_M ($m^3 \cdot mole^{-1}$) in the range 14–300 K and the inverse molar susceptibility in the high-temperature region (>110 K) are shown in Fig. 4. A detailed analysis of the complex behavior of the χ_M curve at low temperatures is beyond the scope of the present paper. A least-squares fit of a line (correlation 0.9998) through the selected high-temperature χ_M^{-1} data gives a Curie constant $C = 8.69(2) \times 10^{-5}$ $m^3 \cdot K \cdot mol^{-1}$ and Weiss temperature $\theta = -132(1)$ K. The negative sign of θ indicates a probable antiferromagnetic ordering at low temperature. The spin-only formula ($C \propto g\sqrt{S(S+1)}$, with $g \approx 2.0$) suggests 6.5 unpaired electrons per formula unit Mn_2OBO_3. The expected number of unpaired electrons can range from three for a complete low-spin state to nine for the high-spin state. This indicates that a significant fraction of the Mn ions are in a high-spin state, in agreement with the observed Mn–O bond lengths (cf. above).

ACKNOWLEDGMENT

The synthetic and structural investigations on metal borates have been financially supported by the Swedish Natural Science Research Council.

REFERENCES

1. Y. Takéuchi, T. Watanabé, and T. Ito, *Acta Crystallogr.* **3,** 98 (1950).
2. J. S. Swinnea and H. Steinfink, *Am. Mineral.* **68,** 827 (1983).
3. R. Norrestam, K. Nielsen, I. Søtofte, and N. Thorup, *Z. Kristallogr.* **189,** 33 (1989).
4. L. A. Harris and H. L. Yakel, *Acta Crystallogr.* **22,** 354 (1967).
5. J. D. Carpenter and S.-J. Hwu, *J. Solid State Chem.* **97,** 332 (1992).
6. R. Chevalier, P. Laruelle and J. Flahaut, *Bull. Soc. Fr. Mineral. Cristallogr.* **90,** 564 (1967).
7. R. Norrestam, *Z. Kristallogr.* **189,** 1 (1989).
8. R. Norrestam, *Acta Chem. Scand.* **21,** 2871 (1967).
9. G. M. Sheldrick, "SHELX-76. Program for crystal structure determination." University of Göttingen, 1976.
10. "International Tables for X-Ray Crystallography," Vol. **IV.** Kynoch Press, Birmingham, 1974.
11. E. Dowty, "ATOMS, A Computer Program for Displaying Atomic Structures." Copyright 1989, Eric Dowty, 521 Hidden Valley Road, Kingsport, TN 37663.
12. M.-H. Whangbo, M. Evain, T. Hughbanks, M. Kertwsz, S. Wijeysekera, C. Wilder, C. Zheng, and R. Hoffmann, "Quantum Chemistry Program Exchange" Program 571, 9 No. 2 (1989) 61. Indiana University, Bloomington, IN, 1989.
13. H. J. Monkhorst and J. D. Pack, *Phys. Rev. B* **13,** 5188 (1976).
14. D. B. Brown, W. H. Crafoord, J. W. Hall, and W. E. Hatfield, *J. Phys. Chem.* **81,** 1303 (1977).
15. P. Moore and T. Araki, *Am. Mineral.* **59,** 985 (1974).
16. V. Venkatakrichnan and M. J. Buerger, *Z. Kristallogr.* **135,** 321 (1972).
17. I. D. Brown and D. Altermatt, *Acta Crystallogr. Sect. B* **41,** 244 (1985).
18. R. Norrestam *Z. Kristallogr.* **209,** 99 (1994).
19. R. D. Shannon, *Acta Crystallogr. Sect. A* **32,** 751 (1976).
20. L. Pauling, "The Nature of the chemical bond," 3rd ed. Oxford Univ. Press, London/New York, 1969.
21. "International Tables for Crystallography," Vol. A, Reidel, Dordrecht, 1983.
22. S. Alvarez, Universitat de Barcelona, unpublished 1989.
23. P. Pyykkö, L. J. Laakkonen, and K. Tatsumi, *Inorg. Chem.* **28,** 1801 (1989).
24. R. Norrestam, M. Kritikos, K. Nielsen, I. Søtofte, and N. Thorup, *J. Solid State Chem.* **111,** 217 (1994).